

Printed September 1982

# Development of a Solar Flux Tracker for Parabolic Trough Collectors

Karlan D. Boultinghouse

Prepared by  
Sandia National Laboratories  
Albuquerque, New Mexico 87185 and Livermore, California 94550  
for the United States Department of Energy  
under Contract DE-AC04-76DP00789



Issued by Sandia National Laboratories, operated for the United States Department of Energy by Sandia Corporation.

**NOTICE:** This report was prepared as an account of work sponsored by an agency of the United States Government. Neither the United States Government nor any agency thereof, nor any of their employees, nor any of their contractors, subcontractors, or their employees, makes any warranty, express or implied, or assumes any legal liability or responsibility for the accuracy, completeness, or usefulness of any information, apparatus, product, or process disclosed, or represents that its use would not infringe privately owned rights. Reference herein to any specific commercial product, process, or service by trade name, trademark, manufacturer, or otherwise, does not necessarily constitute or imply its endorsement, recommendation, or favoring by the United States Government, any agency thereof or any of their contractors or subcontractors. The views and opinions expressed herein do not necessarily state or reflect those of the United States Government, any agency thereof or any of their contractors or subcontractors.

Printed in the United States of America  
Available from  
National Technical Information Service  
U.S. Department of Commerce  
5285 Port Royal Road  
Springfield, VA 22161

NTIS price codes  
Printed copy: A03  
Microfiche copy: A01

SAND82-1600  
Unlimited Release

DEVELOPMENT OF A SOLAR FLUX TRACKER  
FOR PARABOLIC TROUGH COLLECTORS

Karlan D. Boultinghouse  
Solar Research and Evaluation Division 9721  
Sandia National Laboratories  
Albuquerque, New Mexico

ABSTRACT

This report describes the development of a solar flux tracker for application to a parabolic trough solar thermal collector. Tests were conducted at the Collector Module Test Facility and Performance Prototype Trough Test Facility on a resistance wire type solar flux sensor. The device consists of two fine wires installed along each side of the absorber tube parallel to the axis. The wires change resistance as a function of the solar flux arriving at the absorber from the reflectors. The resistance of the two wires is compared to produce a null signal when both wires are equally illuminated. The signal from the wires is used in combination with a microprocessor control system to drive the collectors to the optimum tracking angle. Comparisons are made between the performance of the flux tracker, a computer-based tracker and a shadow band tracker.

#### ACKNOWLEDGMENTS

The author gratefully expresses his appreciation to J. L. Todd, Jr., 9721, R. Schindwolf, 5622, and V. E. Dudley, EG&G, for valuable assistance in testing and development of tracking device.

## CONTENTS

	<u>Page</u>
Introduction . . . . .	7
Description . . . . .	9
Material Environmental Tests . . . . .	11
Tracking Tests and Results . . . . .	14
Preliminary Tests . . . . .	16
Design Tests . . . . .	25
Cost . . . . .	33
Conclusions . . . . .	34
References . . . . .	35

## ILLUSTRATIONS

<u>Figure</u>		<u>Page</u>
1	Flux Wire Sensor as Installed on Performance Prototype Trough . . . . .	10
2	"O"-Ring Collar Assembly . . . . .	13
3	Engineering Prototype Trough Tracking System . . . . .	15
4	Performance Prototype Trough Tracking System . . . . .	17
5	Circuit for Recording Output Signal of Wire Configuration . . . . .	18
6	Results of A and B Configuration Test . . . . .	19
7	Results of C and D Configuration Test . . . . .	20
8	Configuration D Output vs Trough Angle . . . . .	22
9	Flux Wire Differential Output vs Temperature . . . . .	24

## ILLUSTRATIONS (cont)

<u>Figure</u>		<u>Page</u>
10	Typical All-Day Efficiency Plot from Flux Wire Tracking System	26
11	Flux Wire and Computer Tracking Peak Efficiency vs Output Temperature	27
12	String #4 Efficiency vs Solar Time	30
13	Performance Test of Shadow Band, Computer and Flux Wire Tracking	32

## DEVELOPMENT OF A SOLAR FLUX TRACKER FOR PARABOLIC TROUGH COLLECTORS

### INTRODUCTION

Solar collectors that track the sun on only a single axis commonly use one of three different tracking concepts. These are shadow band (indirect view optical tracking), computed sun position tracking, and receiver flux sensor tracking (direct view optical tracking).

Shadow band devices typically utilize two photocells, which are normally separated by a vertical shadow plate. When the device is mounted to the trough and pointed at the sun, the shadow plate shades the photocells equally, resulting in a nulled differential output. If the device is not pointed to the sun, one photocell will be illuminated more than the other. This difference between the cells output is used to drive the trough in the proper direction to reduce the signals to zero. When the tracker is properly aligned with the collector, the solar flux reflected from the trough is focused on the receiver tube.

Shadow band systems track the sun satisfactorily under ideal conditions, but user experience has shown operational problems. Disadvantages of shadow band trackers include

differential aging of the light sensors and dirt or dust on the sensors, both of which cause tracking errors. Unequal light intensity from cloud edges and light reflections from buildings can affect the tracking performance. Master tooling and site specific correction for collectors are required from indirect tracking devices to assure adequate alignment.

When computer tracking is used, the solar position is calculated as a function of time, and the collector is aimed at the calculated position in the sky. A highly accurate angle-measuring device, such as a digital shaft encoder, must be installed on the rotating axis in order to position the collector to the calculated angle. Computer tracking has advantages over the shadow band technique in that light reflections, clouds, varying levels of sunlight, etc., cannot affect tracking accuracy, but equipment costs are much higher.

This report describes the development of an integrating direct view optical resistance wire solar flux sensor. The system combines a microprocessor to calculate the sun's position and then rotates the collectors to the calculated angle. The programmed microprocessor then generates corrections to the calculated angle by seeking the tracking wires null signal. This hybrid tracking control system has advantages over both indirect computer sun angle and shadow band tracking in that the high-cost optical shaft encoder required for computer sun tracking can be replaced with a low-cost inclinometer angle sensing device. Direct tracking sensors generates its tracking signal from incoming concentrated solar flux at the receiver

tube. This method has the potential to minimize the effect of integrate optical imperfections and trough misalignments.

The sensing wires are mounted on the absorber tube, one on each side, 180 degrees apart, parallel to the axis of the trough. Incoming solar flux from the reflector heats the wires and changes their resistance. A sensing circuit detects the change in wire resistance and generates a voltage proportional to the resistance change which is then used for tracking.

#### DESCRIPTION

The solar flux wire tracker was designed for use on parabolic-cylindrical solar collectors. Figure 1 shows the wires installed on the Performance Prototype Trough (PPT). Major components of the device are two nickel wires, spring clips with insulators, expansion springs, feed-through insulators and jumper wires.

Type 201, 0.005-inch diameter uninsulated nickel wires were installed as the sensing device for the tracker. Nickel has good mechanical strength, reasonable thermal conductivity, high resistance to corrosive atmospheres and ease of joining itself to other metals. Elgiloy (an alloy of nickel, iron, chromium, and cobalt) was selected to fabricate the spring clip and expansion spring. Elgiloy is suitable for temperatures from sub-zero to 900 degrees F. The alloy has less than 1.5% relaxation at stress levels of 75 Ksi and at temperatures below 850 degrees F.

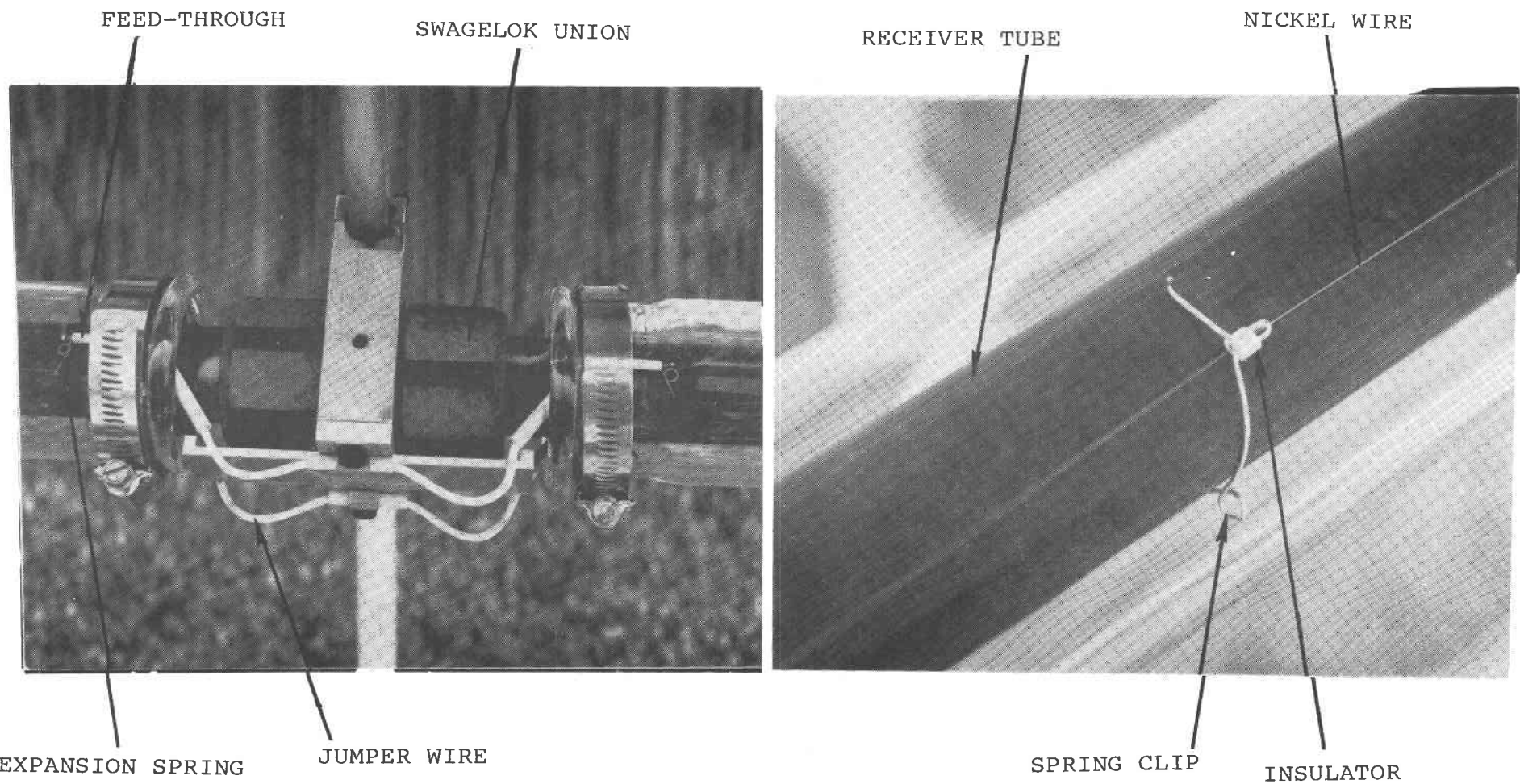


Figure 1. Flux wire sensor as installed on Performance Prototype Trough.

The spring clip provides both alignment and spacing for the sensing wire. Mullite oval, double-bore ceramic tubing was used to provide electrical insulation for the nickel wires. Ceramaseal [1] subminiature feed-through insulators were laser welded into the stainless-steel receiver tube "O"-ring collar. The wires and other components are capable of continuous operation in air at 900 degrees F.

The feed-through insulators are high-alumina ceramic and the metal sleeves are nickel. The flux sensing wires are terminated at the expansion/torsion spring with BAG-7 silver solder. The spring maintains tension on the sensing wires and prevents overstress during thermal cycling. The jumper wire between receiver tubes uses #22 AWG nickel, high-temperature, fire-resistant wire, and can operate continuously at 800 degrees F. BAG-7 silver solder is again used to join the jumper wires at the feed-through insulators. Ceramic tubing is placed over the jumper wire and feed-through junction to prevent shorting. A loop at each end of the jumper wire relieves stress on the feed-through junction.

#### MATERIAL ENVIRONMENTAL TESTS

Environmental tests were conducted on the material selected for the tracker sensing wire assembly. Under normal operation the components were subjected to temperature cycling from ambient to 650 degrees F., humidity and UV radiation.

The first test was conducted on the "O"-ring collar assembly as shown in Figure 2. The nickel base of the feed-through is laser spot welded into 304 stainless collar and the expansion spring welded (TIG) to the end of the nickel wire conductor of the feed-through. Ten assemblies were then placed in an environmental test chamber and programmed to cycle from ambient to 650 degrees F, with relative humidity to 100%. A total of 150 cycles was run on the ten assemblies. At intervals of ten cycles each assembly was microscopically inspected for failure and oxidation. The results of this test showed one failure at the welded laser joint between the feed-through and collar. This failure was the result of a poor mechanical fit at the interface resulting in an improper fuse of the laser weld. A light coherent oxide was observed after the first ten cycles on the expansion spring, but further cycling showed no increase in the oxide film or any detrimental effect on the material or weld joints.

The second environmental test was designed to examine the compatibility of the BAG-7 silver solder with that of nickel sensing wire and Elgiloy expansion spring. Ten joints were made using BAG-7 and an inorganic acid flux. The assemblies were placed in a furnace at 700 degrees F for 720 hours and air cooled to room temperature, then inspected for environmental damage. The inspection results showed that the surface of all three materials in the assembly was covered with an incoherent black residue and showed evidence of chemical attack.

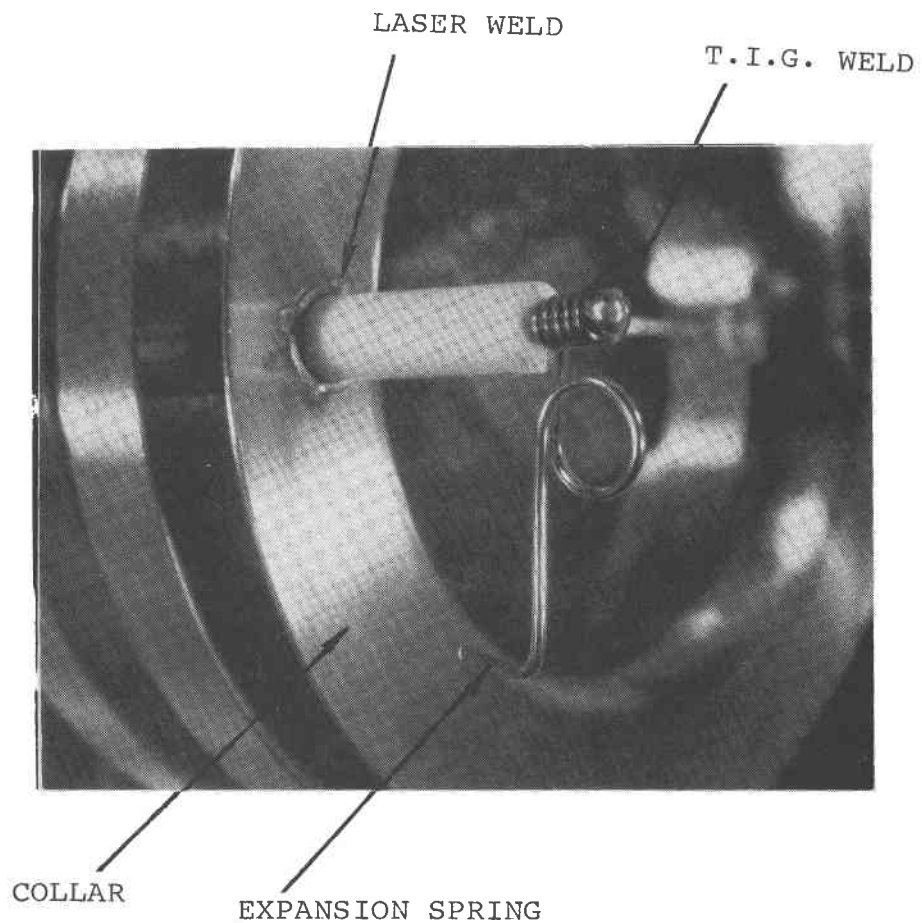


Figure 2. "O"-ring collar assembly.

The chemical analysis of the black residue showed that it was decomposed silver solder flux, which contains acid and salts resulting in the attack of the material in the assembly. This test concluded that cleaning of the joint is a requirement before environmental exposure.

#### TRACKING TESTS AND RESULTS

The preliminary tests of the resistance wire tracking system were run at the Collector Module Test Facility (CMTF). The tracking system was installed on the Sandia Mod. 2 Engineering Prototype Trough (EPT-2) [2]. The EPT-2 collector used two 2 m x 6 m troughs and four 25 mm (1 inch diameter x 3 m long) receiver tubes.

The development of a tracking system designed to incorporate both computer and flux sensor tracking is shown in Figure 3. The system can compare the collector position as controlled by the computer to the tracking signal from the resistance wire flux sensor. The test was designed to obtain basic data and understanding of the problems and advantages associated with using the hot wire flux sensor concept.

The design test was run at the Performance Prototype Trough Test Facility [3]. The PPT installation uses four drive strings, each having four 2 m x 6.1 m reflectors. The PPT receiver used eight receiver tubes, each 31.75 mm (1.25 inch) diameter x 3 m long. The total length of the PPT collector system is 97.5 meters. A Honeywell-designed, microprocessor-based

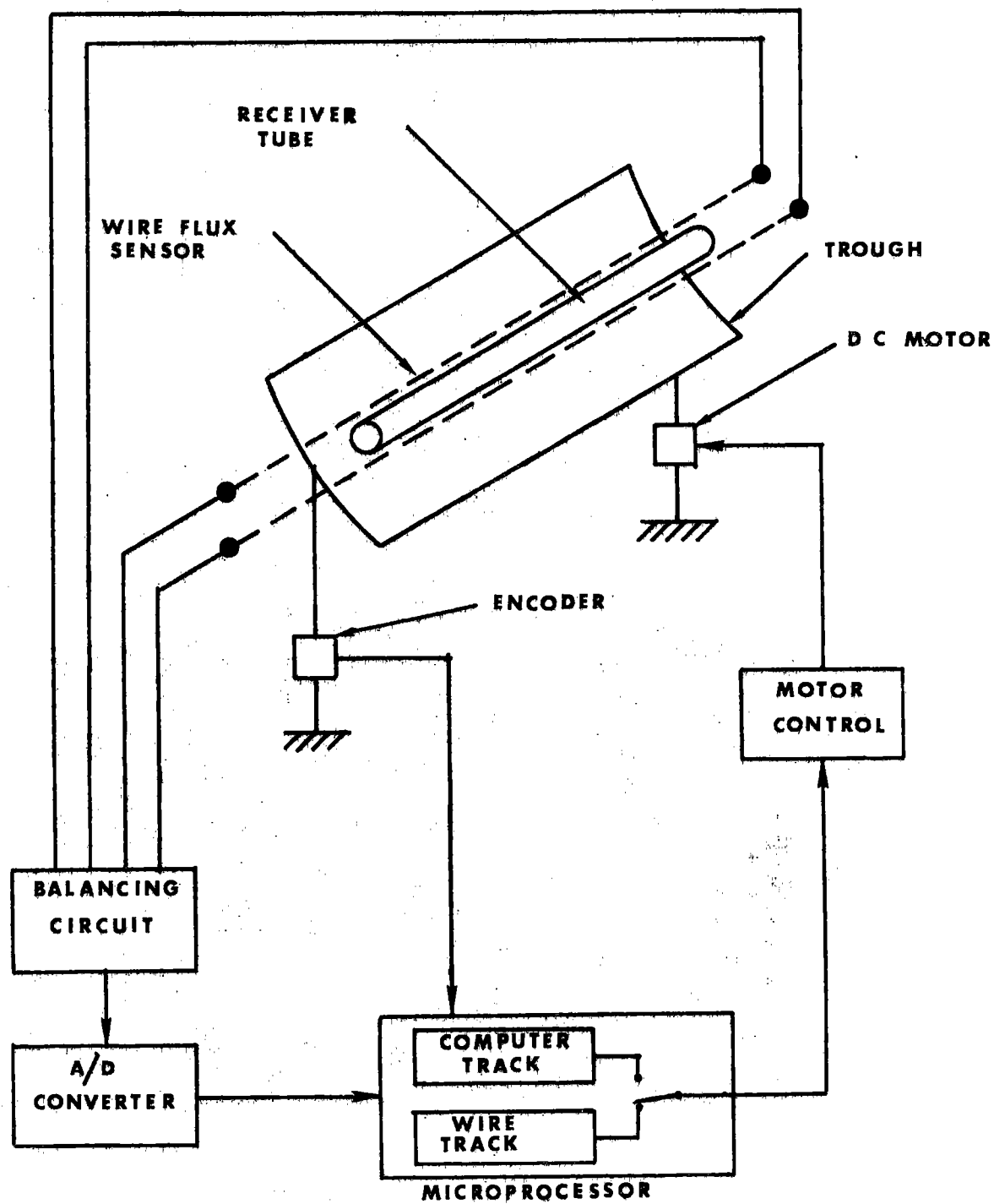


Figure 3. Engineering Prototype Trough Tracking System.

tracking and control system was installed on each collector string. The hardware and software design combined rough calculated sun-angle tracking with wire flux tracking. A schematic of the system is shown in Figure 4. The purpose of this test was to install the sensor on a larger collector field to obtain performance, reliability and material compatibility data.

#### Preliminary Tests

To obtain a better understanding of the output signal response of the heat flux sensor, four different configurations of the resistance wire were investigated. Each configuration was installed on a 3 m length of receiver tube for testing.

Voltage output from the resistance wire flux sensor was recorded as the receiver was driven slowly through the focused sunlight from the collector. Figure 5 shows the circuit used to record the electrical output of each individual wire, and the differential signal output of the two wires. Before each test, the bridge circuit was balanced at ambient temperature with collectors in stow. Figures 6 and 7 show the results obtained from each configuration study.

Configurations A, B, and C show that the best focus for optimum tracking occurred when the voltage output was less than maximum. However, configuration C and D shows that increased wire spacing caused optimum focus to occur at the wire's maximum voltage output with a resulting difference signal that is adequate for tracking. A tracking envelope similar to that shown for A, B, and C was reported in previous

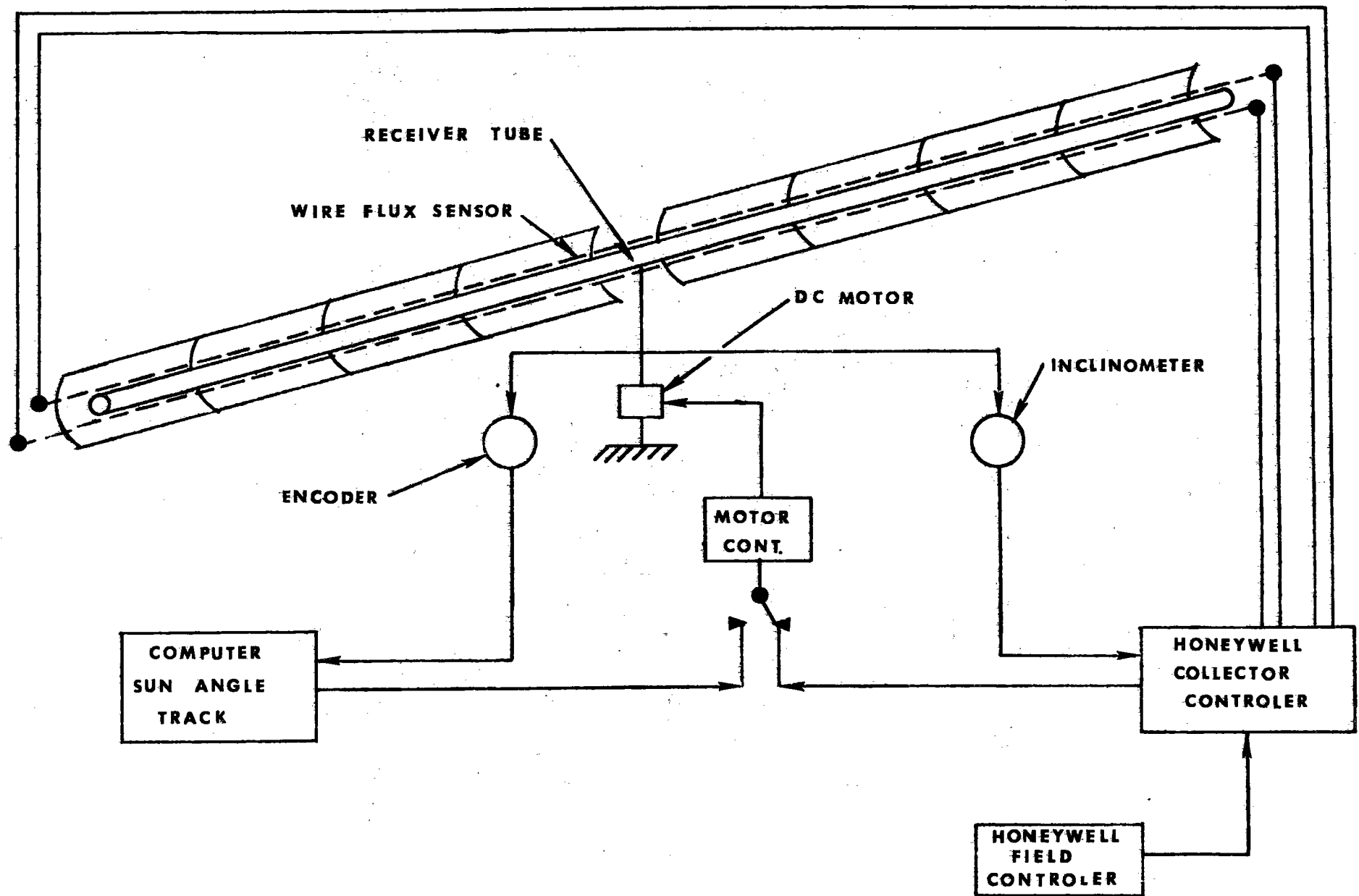


Figure 4. Performance Prototype Trough Tracking System.

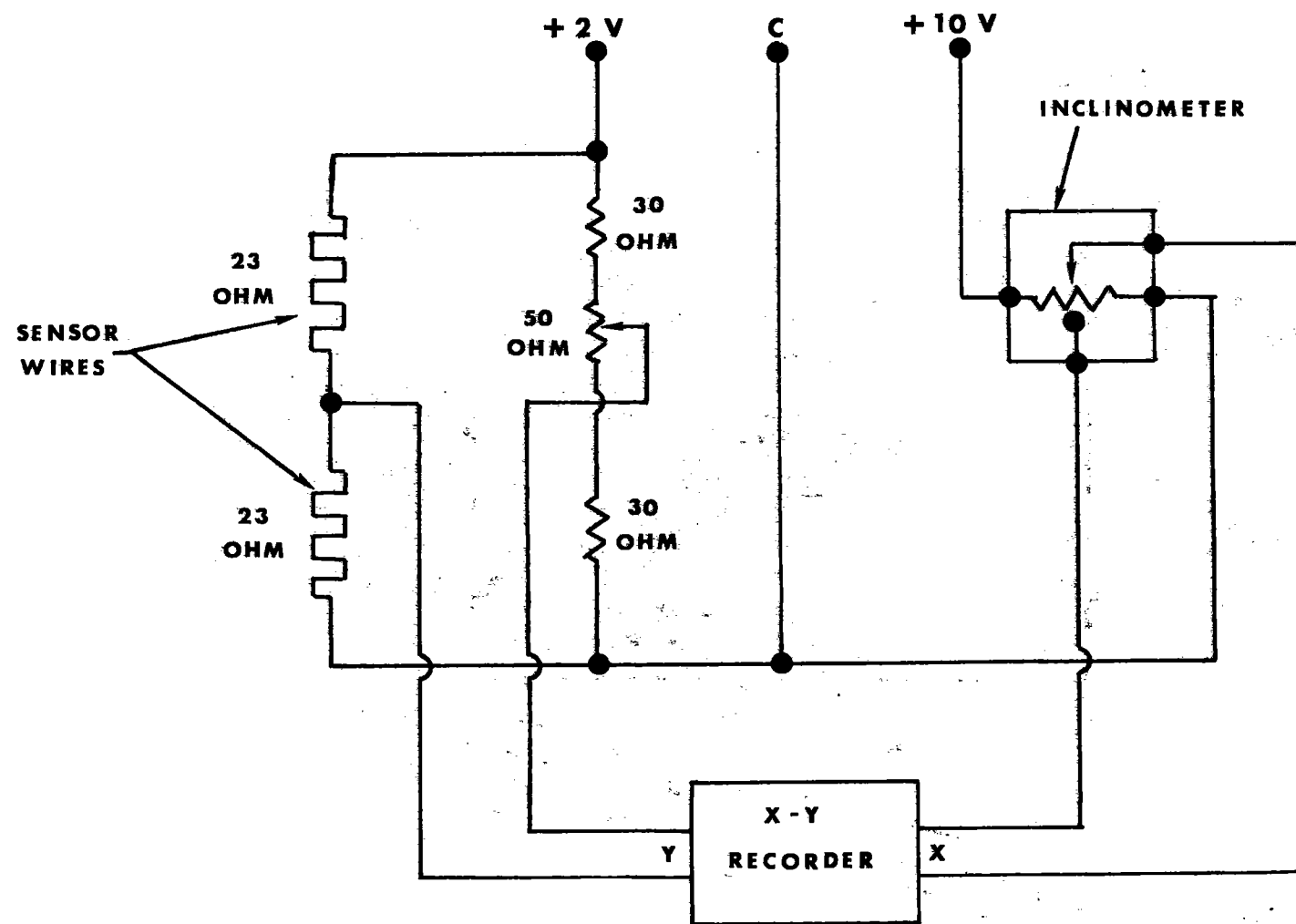
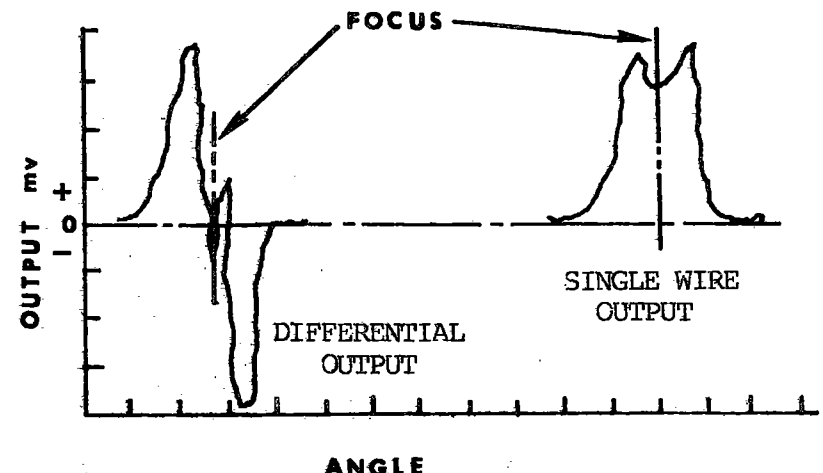
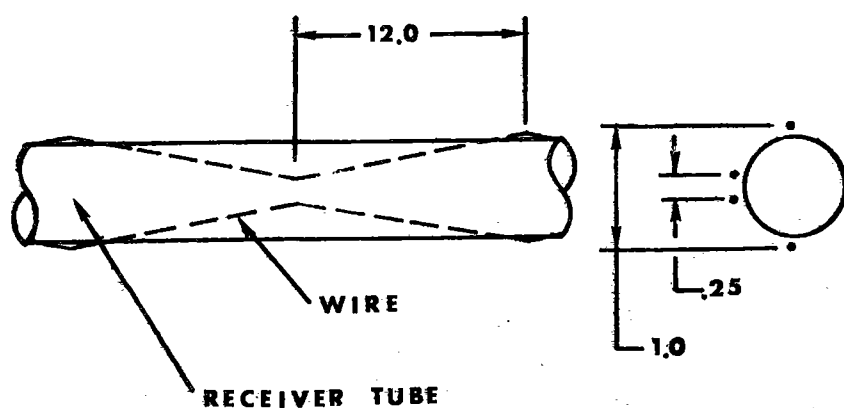
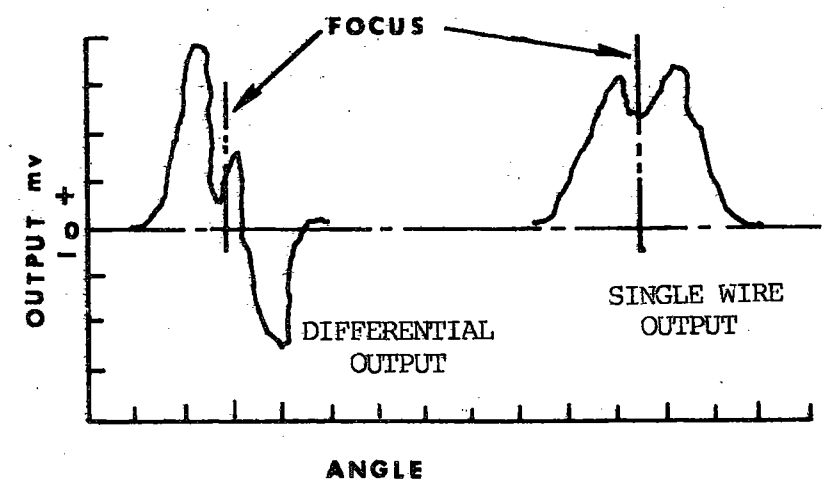
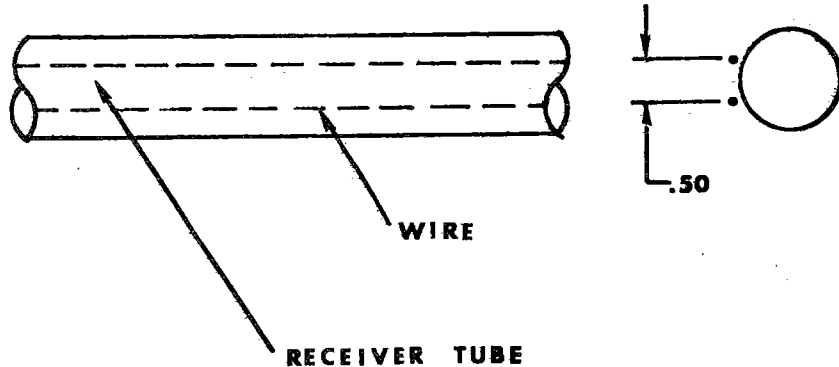


Figure 5. Circuit for recording output signal of wire configuration.

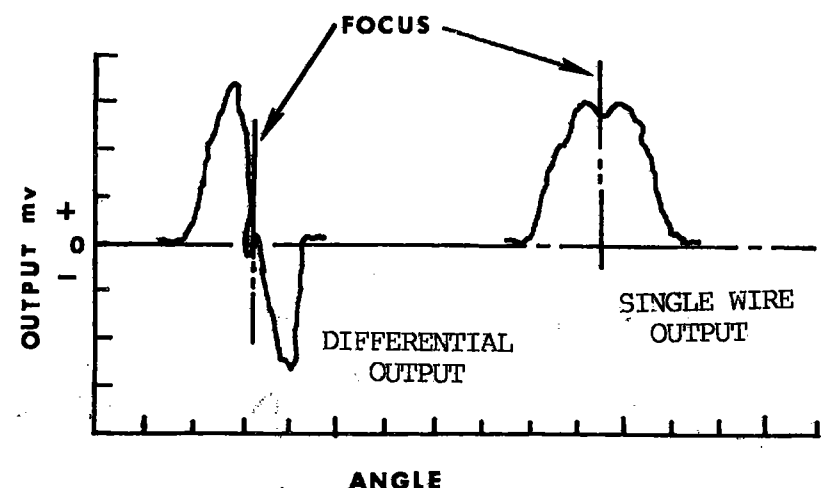
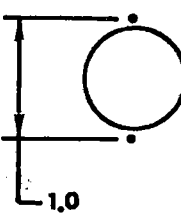
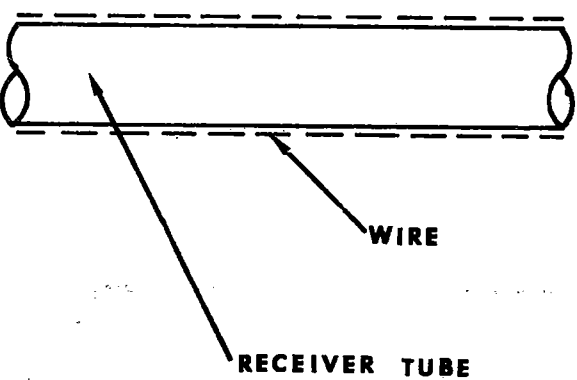
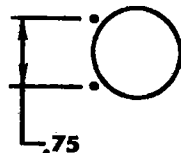
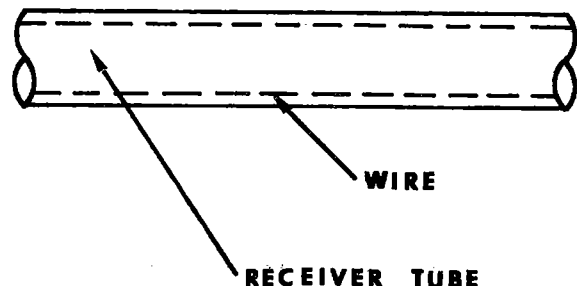


(A)

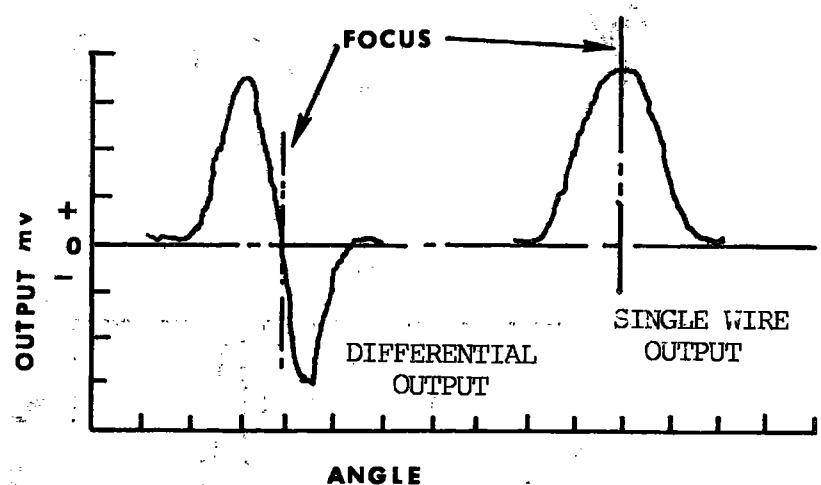


(B)

Figure 6. Results of A and B configuration test.



(C)



(D)

Figure 7. Results of C and D configuration test.

tests by Kohler and Wilcoxen [4]. The results of this test show that the single-peak envelope signal from configuration D (Figure 8) would provide sufficient output and sensitivity for accurate tracking.

For the first operational test, configuration D of the flux sensor was installed on the first 3 m length of receiver tube at the east end of the EPT collector. Good tracking signals were obtained during the middle of the day, but low signal output was recorded at early morning start-up. The high angle of incidence of solar beam radiation during the early morning caused most of the reflected light from the collector's mirrors to fall on the receiver well to the west of the illuminated position at solar noon. Only about 25% of the east 3 m of receiver was illuminated. The wire flux sensor was removed and installed on the second 3 m tube. This provided 100 percent illumination at an angle of incidence of 70 degrees and excellent tracking signals throughout the day.

During initial testing, the signal from the resistance wire flux sensor showed an angle offset from the tracking null which varied with both operating temperature and time-of-day. The tracking signal offset resulted in a tracking error of 0.6 degrees at 300 degrees C fluid temperature at various times during the day. A tracking error of no more than 0.2 degrees is required to insure that all the reflected light will fall on the receiver at all hours of the day. Further testing was conducted to investigate the causes of the tracking signal offset and the resulting collector tracking errors.

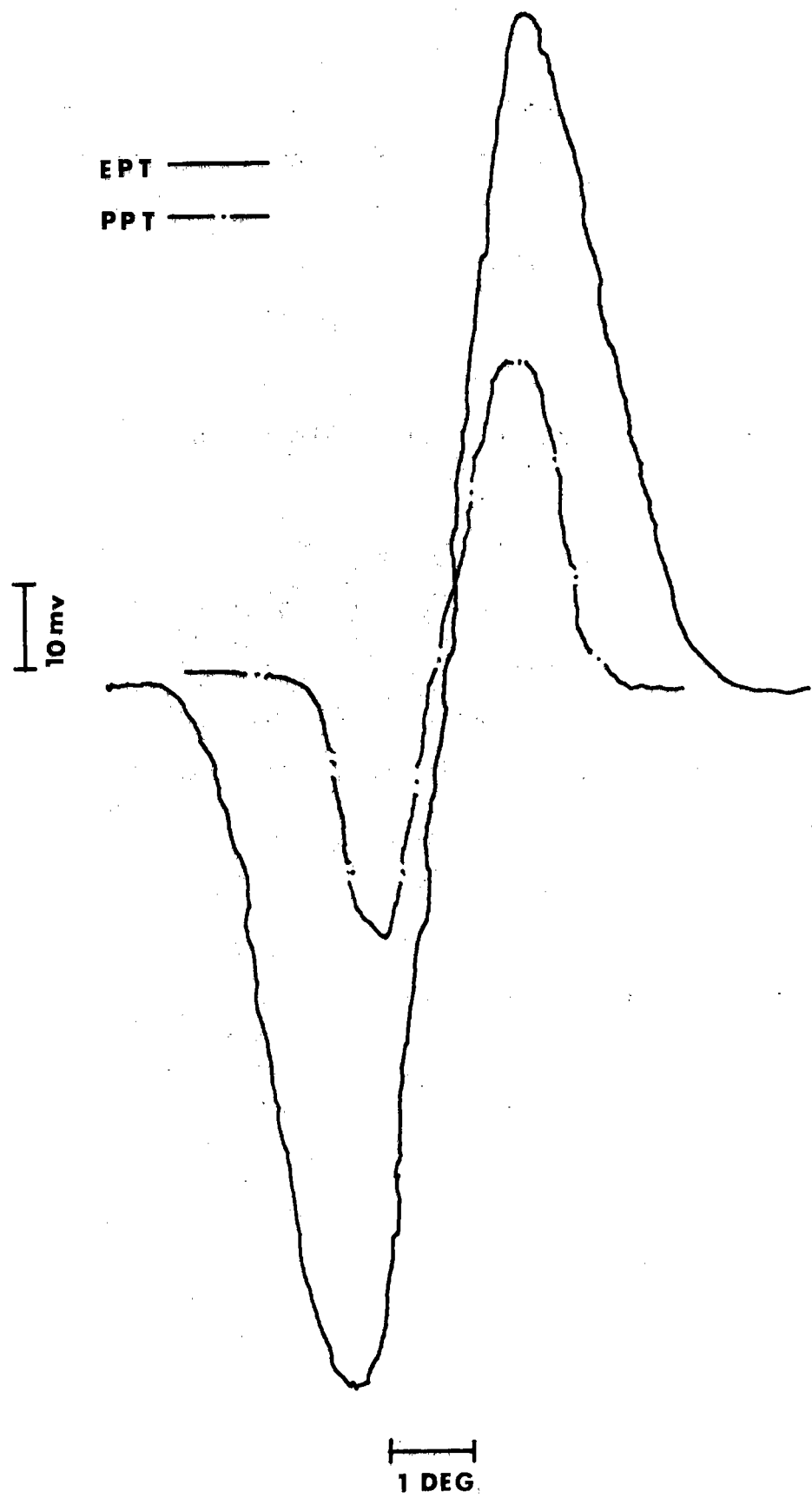


Figure 8. Configuration D Output vs Trough Angle

The fluid temperature in the receiver was stabilized at ambient air temperature with the collector out of focus and at 100, 200 and 300 degrees Celsius. At each temperature, the collector was positioned at 90 degrees south, horizontal and 90 degrees north and the differential output of the wire flux tracker was recorded. The results are shown in Figure 9. The data shows that the flux sensor offset angle is dependent on trough angle and fluid temperature, both of which affect the temperature distribution within the receiver tube. The tracking offset angle is most likely caused by convection air currents within the receiver annulus unequally heating the two resistance wires. The effects of natural air convection in annular receiver tubes have been reported by Hickox and Gartling [5].

From the data in Figures 8 and 9, an offset angle algorithm was written:

$$\Delta\theta = K_4 \left\{ \epsilon + [K_3 + K_2 (T - K_1) \cos \theta] \right\}$$

From curve:

$K_1 = 5^\circ\text{C}$  (offset)  $T = \text{fluid temperature } (\text{ }^\circ\text{C})$

$K_2 = .466 \text{ mv/ } ^\circ\text{C}$  (slope)  $\epsilon = \text{error signal from wire (mv)}$

$K_3 = 10 \text{ mv}$  (offset)  $\theta = \text{collector angle from horz. (deg.)}$

$K_4 = .007 \text{ DEG}'\text{s/mv}$  (slope)  $\Delta\theta = \text{error in trough position (deg.)}$   
from tracking wire  
output single

The offset angle algorithm was inserted into the wire sensor tracking software. Peak efficiency data was obtained

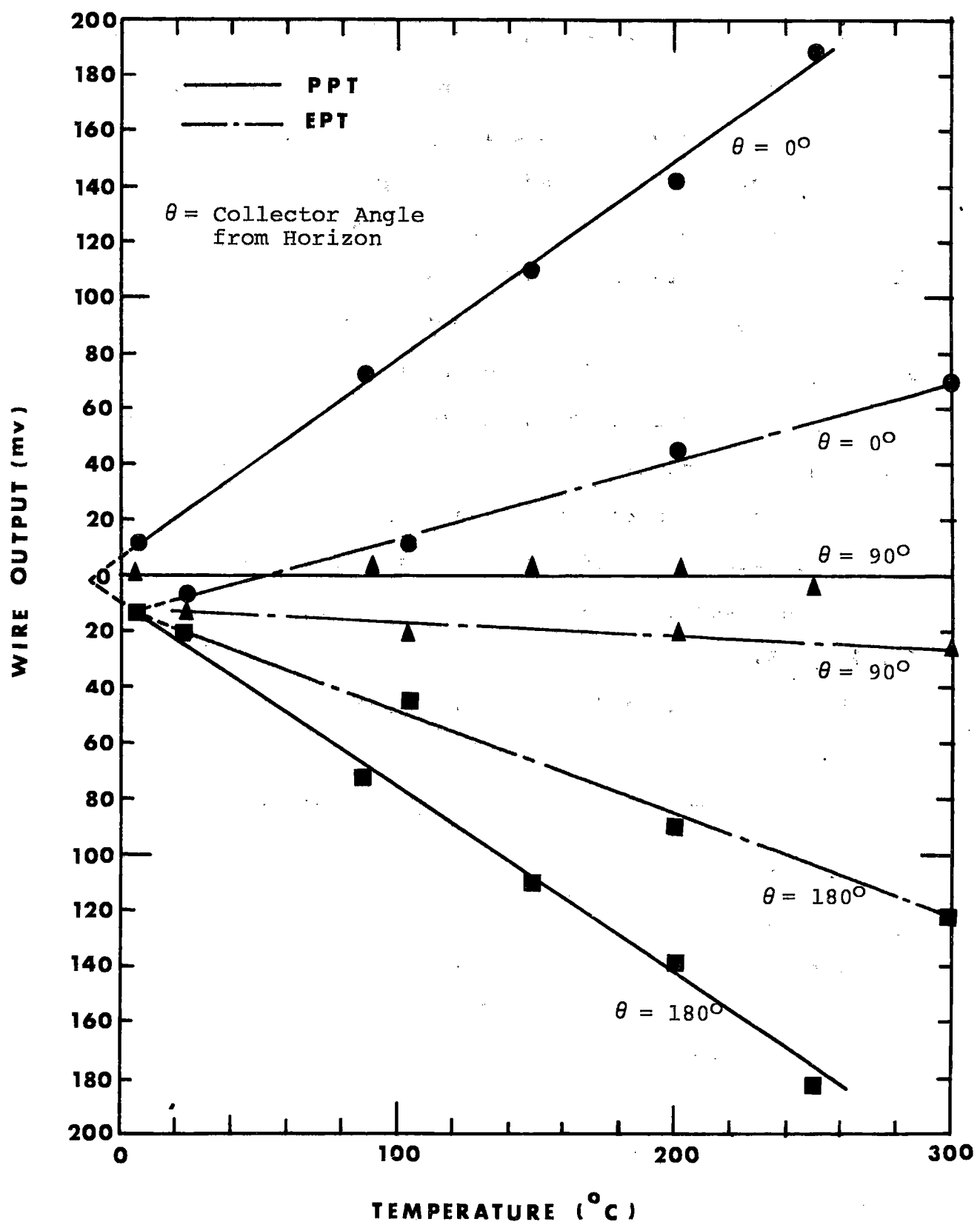


Figure 9. Flux wire differential output vs. fluid temperature.

at approximately 100, 200 and 300 degrees Celsius. A typical all-day efficiency plot from flux wire tracking is shown in Figure 10.

Peak efficiency vs output temperature for both flux wire and computer tracking is shown in Figure 11. The plot shows that efficiency of the collector decreases as the temperature is increased; the decrease in efficiency is caused by increasing thermal losses from the receiver. Both tracking methods produced approximately the same collector efficiencies.

#### Design Tests

After establishing the basic design and operating characteristics of the wire sensor from the preliminary tests, configuration D was installed on the PPT collector field. A fixture was designed to insure proper alignment of the resistance wires with the trough. The fixture also provided a tool for assembling receiver tube hardware.

The position of each wire was measured from the Swagelok [6] tube fitting body hex flats that were installed into the receiver tube support yoke. This method provided the required alignment of the sensing wires to the troughs for the 32 receiver tubes. Field installation of the jumper wires completed the assembly installation of the solar flux tracking wires.

PPT system component checkout was conducted using calculated sun angle computer tracking. The system was operated for approximately 60 hours at fluid temperatures between ambient and 300 degrees Celsius. Upon completion of system

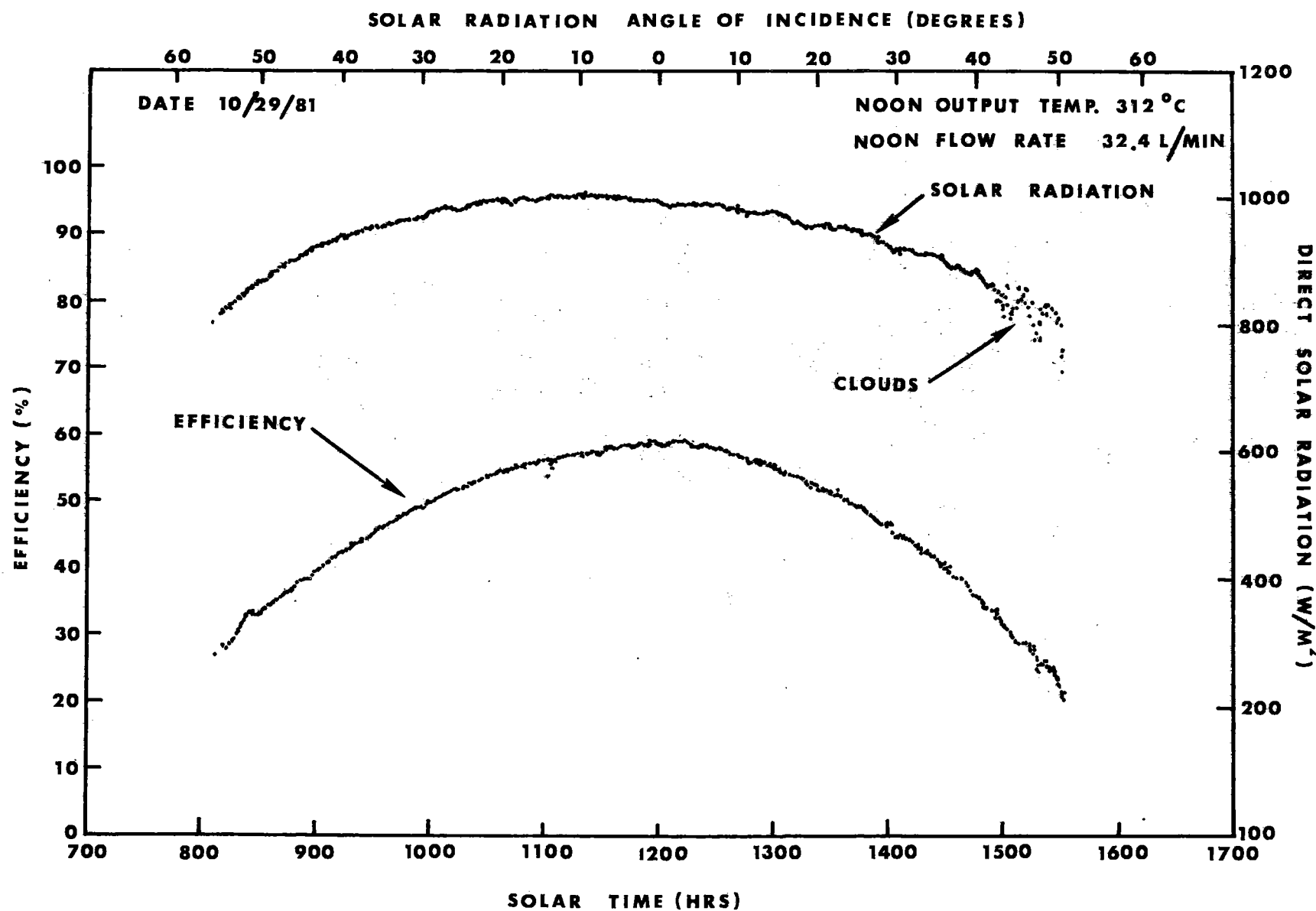


Figure 10. Typical all-day efficiency plot from flux wire tracking system.

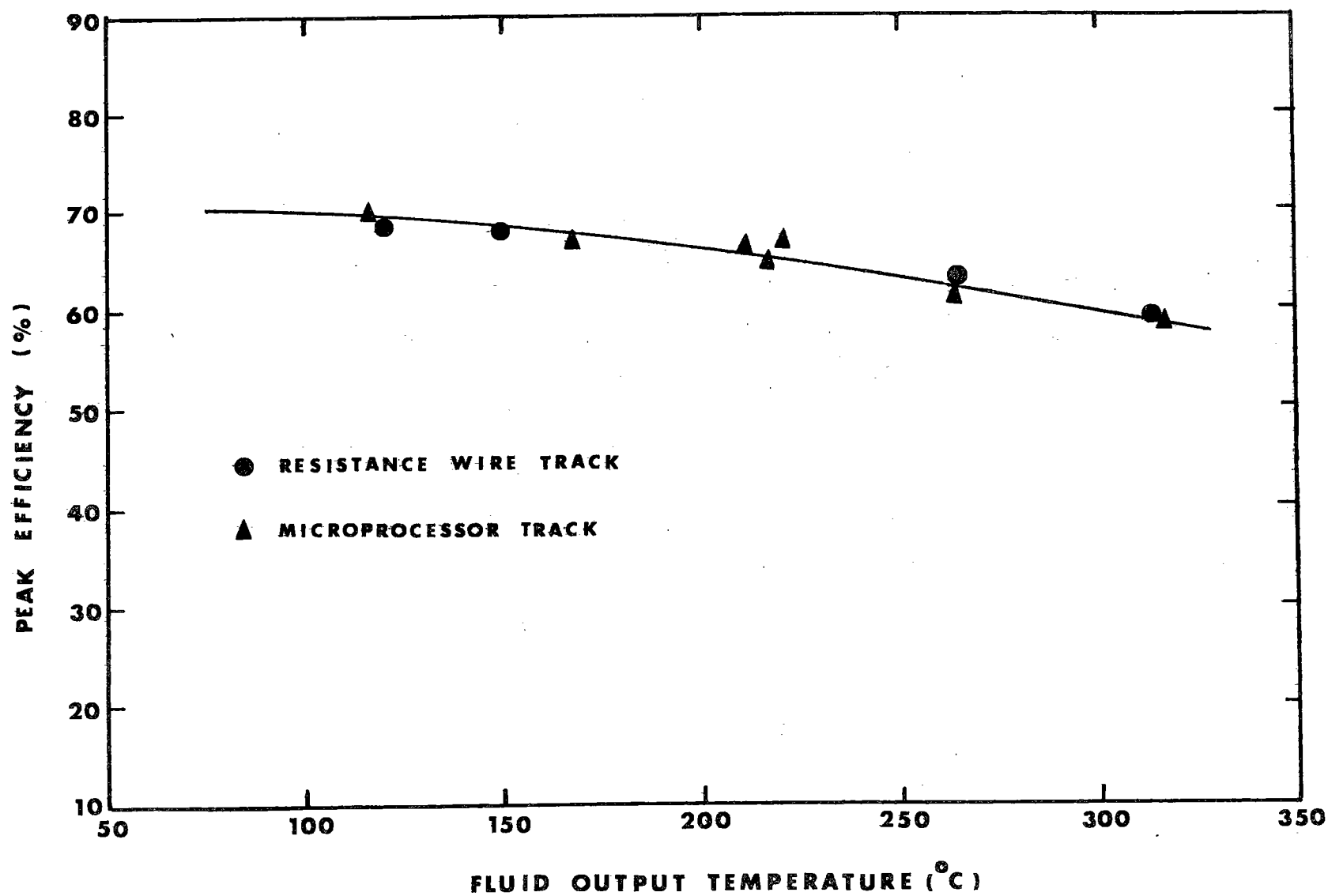


Figure 11. Flux wire and computer tracking peak efficiency vs. output temperature.

tests, the components of the flux sensor were inspected. Several of the Mullite insulators located in the center of five receiver-tube assemblies had fractured. The fractures are probably due to sagging of the metal receiver tubes (which was observed during assembly, prior to operation at elevated temperature) and from movement caused by temperature cycling and torque load from the flexible receiver tube hose assembly. Receiver tube movement crushed the insulators between the glass tubing inside diameter and metal tubing outside diameter. Due to the unavailability of spare parts, repair of all fractured insulators was not possible. Solar flux tracking was, therefore, studied using only three of the four collector drive strings.

The resistance wire signals were electrically balanced at ambient temperature with the three collector drive strings in the horizontal position (reflectors aimed at the zenith). The offset angle algorithm used with PPT was derived from string #4 and the results are shown in Figure 9. From the curves in Figures 8 and 9, the offset angle for the PPT collector field was written:

$$\Delta\theta = K_4 \left\{ \epsilon + [K_3 + K_2 (T - K_1) \cos \theta] \right\}$$

From Curve:

$K_1 = -15^\circ\text{C}$ (offset)	$T = \text{fluid temperature } (\text{ }^\circ\text{C})$
$K_2 = .722 \text{ mv/ } ^\circ\text{C}$ (slope)	$\epsilon = \text{error signal from wire (mv)}$
$K_3 = 0.0 \text{ mv}$ (offset)	$\theta = \text{collector angle from horz. (deg.)}$
$K_4 = .025 \text{ DEG's/mv}$ (slope) from tracking wire output single	$\Delta\theta = \text{error in trough position (deg.)}$

The offset angle data from the PPT collector field shows a symmetrical curve pattern about the axis of the plot, while the data from the EPT-2 (Figure 9) shows an offset of the curves. The improved symmetry obtained on the PPT installation was due to the more precise location of the tracking wires that resulted from using an improved assembly fixture.

After inserting the offset angle algorithm into the Honeywell collector control system, an all-day efficiency test was conducted on the flux wire tracker. The results of this test from string #4 are shown in Figure 12. The DELTA-T string established thermal equilibrium at 0830 solar time and an output temperature of 585 degrees F. The solar flux tracker system maintained stable tracking to 1630 hours, at which time the angle of incidence was 67 degrees and solar radiation normal to the trough was 325 (W/m<sup>2</sup>).

A test was designed to demonstrate the performance of the flux wire sensor tracking system with that of computer and shadow band tracking.

In the computer-control tracking technique, the calculated tracking angle could change from the ideal tracking angle because of misalignment and imperfections in the collector's string. The PPT computer angle error offset was determined by measuring the system fluid temperature rise as a function of angle. The measured angle error offset was then inserted into the computer software to provide peak efficiency computer tracking for the PPT configuration. A shadow band tracking device was mounted to string #4 of the PPT configuration and, for the same reason

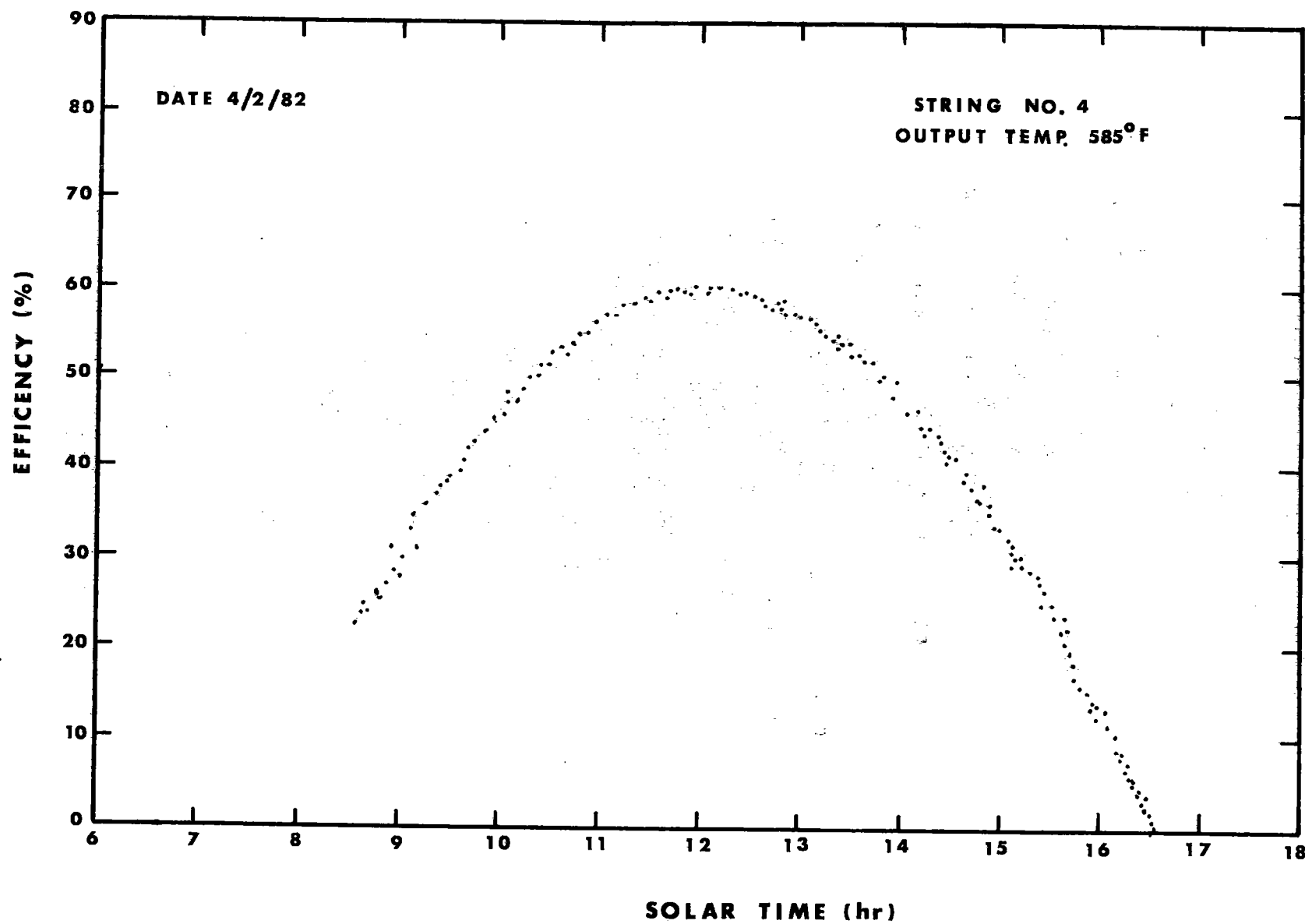


Figure 12. String #4 efficiency vs. solar time.

given above, the optimum tracking angle may differ from the calculated angle. Therefore, the device was adjusted for null at 0900, 1200 and 1500 hours solar time for three consecutive days to insure the best possible alignment. No alignment or adjustment was made on the flux wire sensor.

Tracking of string #4 was switched between the three tracking modes at intervals of approximately 15 minutes during the test day. The results of the test are shown in Figure 13. The shadow band tracking curve indicates a continual efficiency loss throughout the day. Imperfections such as optical quality of the reflector, sagging of the receiver tube, misalignments between the shadow band and reflector and reflector and foundation are the results of efficiency loss for the shadow band tracking. The efficiency curves for both flux wire and fine-tuned computer tracking modes show no difference in the tracking performance of the collector string, but with aging of the collector string such as warping of collector components and foundation movement would require the computer angle offset to be tested and adjusted to maintain peak efficiency. The as-installed flux wire sensor showed the ability to integrate imperfections from the collector components by direct view tracking from the incoming heat flux of the collector.

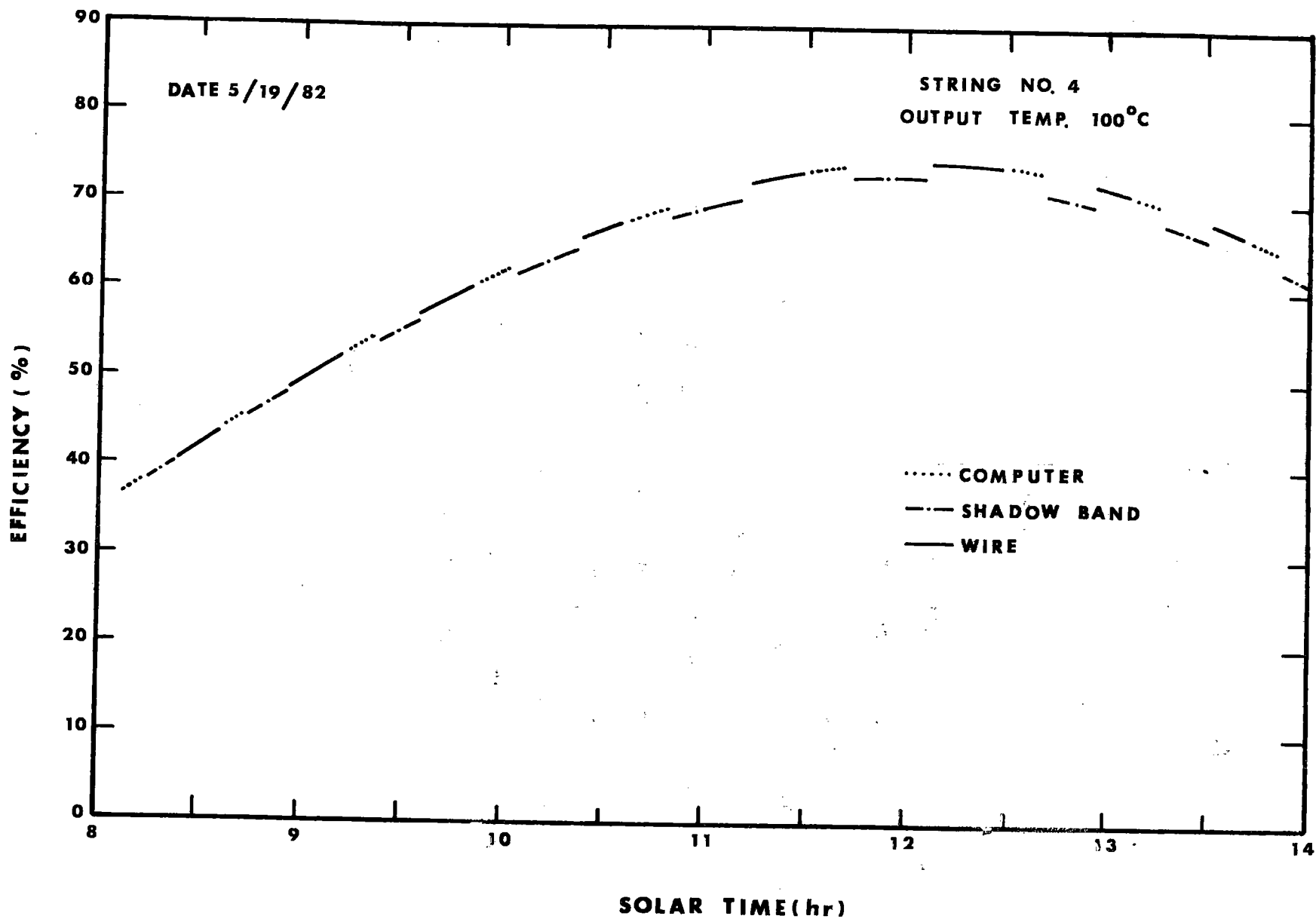


Figure 13. Performance test of shadow band, computer, and flux wire tracking.

## COST

It has been generally accepted that computer sun position tracking be utilized as the tracking device for most single-axis parabolic collectors. For this reason, a cost estimate of the two systems has been compared. The estimated cost is based on one drive string from a large collector array of 24 strings. The results are shown in Table I.

Table I

Item	Computer	Flux Wire
Sensor fabrication	--	40.00
Sensor installation	--	320.00
Optical encoder	1200.00	--
Inclinometer	--	300.00
Field controller	100.00	75.00
Collector controller	500.00	400.00
Wiring	300.00	200.00
Efficiency (adjustment)	100.00	--
String (alignment)	150.00	75.00
Tooling	200.00	--
 TOTAL	 \$2550.00	 \$1410.00

It is expected that with manufacturing development, the cost in Table I would be reduced substantially.

## CONCLUSIONS

A solar flux wire tracker has been developed and tested that allows accurate tracking of parabolic-cylindrical solar collectors. A microprocessor control system is used in combination with the flux wire output signal to drive the collectors to optimum tracking angle.

Environmental tests were conducted on the flux sensor components. The tests resulted in the solution of two potential problems, that of poor fit between collar and feed-through and chemical attack of nickel wire and expansion spring.

The preliminary and design test data established wire sensor configuration, offset angle algorithm and tracking performance for the flux wire tracking system. The direct view tracking device provided the optimum tracking angle by integrating misalignments from the collector's components.

The estimated total cost of the system when compared with computed sun angle tracking was reduced by 45%, mainly due to component and maintenance cost of the system.

## REFERENCES

1. Ceramaseal, Inc. (subsidiary of Interpace) New Lebanon, New York 12126.
2. K. D. Bergeron, R. L. Champion, and R. W. Hunke, editors, "Line-Focus Solar Thermal Energy Technology Development FY 79 Annual Report for Department 4720," SAND80-0865, pp. 18-23.
3. R. L. Champion, editor, "Proceedings of the Line-Focus Solar Thermal Energy Technology Development, A Seminar for Industry," SAND80-1666, Session V - Line-Focus Component Development.
4. S. M. Kohler and J. L. Wilcoxen, "Development of a Microprocessor-Based Sun-Tracking System for Solar Collectors," SAND79-2163, 1979.
5. C. E. Hickox and D. K. Gartling, "The Effects of Non-uniformities on Natural Convection in Annular Receiver Geometries," SAND77-1641, 1977.
6. Crawford Fitting Company, 29500 Solon Road, Solon, Ohio 44139.

**Distribution:**

AAI Corporation  
P.O. Box 6787  
Baltimore, MD 21204

Acurex Aerotherm (2)  
485 Clyde Avenue  
Mountain View, CA 94042  
Attn: J. Vindum  
H. Morse

Advanco Corporation  
999 N. Sepulveda Blvd.  
Suite 314  
El Segundo, CA 90245

Alpha Solarco  
1014 Vine Street  
Suite 2230  
Cincinnati, OH 45202

Budd Company (The)  
Fort Washington, PA 19034  
Attn: W. W. Dickhart

Budd Company (The)  
Plastic R&D Center  
356 Executive Drive  
Troy, MI 48084  
Attn: J. N. Epel

Corning Glass Company (2)  
Corning, NY 14830  
Attn: A. F. Shoemaker  
W. Baldwin

Custom Engineering, Inc.  
2805 South Tejon Street  
Englewood, CO 80110

Donnelly Mirrors, Inc.  
49 West Third Street  
Holland, MI 49423  
Attn: J. A. Knister

Energetics  
833 E. Arapahoe Street  
Suite 202  
Richardson, TX 85081  
Attn: G. Bond

E-Systems, Inc.  
Energy Tech. Center  
P.O. Box 226118  
Dallas, TX 75266  
Attn: R. R. Walters

Ford Motor Company  
Glass Div., Technical Center  
25500 West Outer Drive  
Lincoln Park, MI 48246  
Attn: V. L. Lindberg

General Motors  
Harrison Radiator Division  
Lockport, NY 14094  
Attn: L. Brock

Haveg Industries, Inc.  
1287 E. Imperial Highway  
Santa Fe Springs, CA 90670  
Attn: J. Flynt

Jacobs Engineering Co.  
251 South Lake Avenue  
Pasadena, CA 91101  
Attn: H. Cruse

Jet Propulsion Laboratory (3)  
4800 Oak Grove Drive  
Pasadena, CA 91103  
Attn: J. Becker  
J. Lucas  
V. C. Truscello

McDonnell-Douglas Astronautics  
Company (2)  
5301 Bolsa Avenue  
Huntington Beach, CA 92647  
Attn: J. Rogan  
D. Steinmeyer

New Mexico State University  
Solar Energy Department  
Las Cruces, NM 88001

Distribution (cont)

Owens-Illinois  
1020 N. Westwood  
Toledo, OH 43614  
Attn: Y. K. Pei

PPG Industries, Inc.  
One Gateway Center  
Pittsburg, PA 15222  
Attn: C. R. Frownfelter

Parsons of California  
3437 S. Airport Way  
Stockton, CA 95206  
Attn: D. R. Biddle

Schott America  
11 East 26th Street  
New York, NY 10010  
Attn: J. Schrauth

Solar Energy Information Center  
1536 Cole Blvd.  
Golden, CO 80401  
Attn: R. Ortiz

Solar Energy Research  
Institute (2)  
1617 Cole Blvd.  
Golden, CO 80401  
Attn: B. L. Butler  
B. P. Gupta

Solar Kinetics, Inc.  
P.O. Box 47045  
Dallas, TX 75247  
Attn: G. Hutchison

W. B. Stine  
1230 Grace Drive  
Pasadena, CA 91105

Sunpower Systems  
510 S. 52 Street  
Tempe, AZ 85281  
Attn: W. Matlock

Suntec Systems, Inc.  
2101 Wooddale Drive  
St. Paul, MN 55110

Texas Tech University  
Dept. of Electrical Eng'g.  
P.O. Box 4709  
Lubbock, TX 79409  
Attn: J. D. Reichert

3M-Decorative Products Div.  
209-2N 3M Center  
St. Paul, MN 55144  
Attn: B. Benson

3M-Product Development  
Energy Control Products  
207-1W 3M Center  
St. Paul, MN 55144  
Attn: J. R. Roche

Toltec Industries, Inc.  
40th and East Main  
Clear Lake, IA 50428  
Attn: D. Chenault

U. S. Department of Energy (3)  
Albuquerque Operations Office  
P.O. Box 5400  
Albuquerque, NM 87185  
Attn: G. N. Pappas  
J. A. Morley  
J. Weisiger

U. S. Department of Energy (8)  
Division of Solar Thermal  
Technology  
Washington, DC 20585  
Attn: W. W. Auer  
G. W. Braun  
J. E. Greyerbiehl  
B. Hochheiser  
C. McFarland  
J. E. Rannels  
F. Wilkins (2)

U. S. Department of Energy  
San Francisco Operations Office  
1333 Broadway, Wells Fargo Bldg.  
Oakland, CA 94612  
Attn: R. W. Hughey

Distribution (cont)

University of New Mexico (2)  
Department of Mechanical Eng'g.  
Albuquerque, NM 87113  
Attn: W. W. Wilden  
W. A. Cross

Viking  
3467 Ocean View Blvd.  
Glendale, CA 91208  
Attn: G. Goranson

400 R. P. Stromberg  
1550 F. W. Neilson  
2540 K. L. Gillespie  
5520 T. B. Lane  
5622 R. Schindwolf  
5810 R. G. Kepler  
5820 R. E. Whan  
5840 N. Magnani  
8214 M. A. Pound  
8430 R. C. Wayne  
8431 K. Wally  
8453 W. G. Wilson  
9000 G. A. Fowler  
9700 E. H. Beckner  
9720 D. G. Schueler  
9721 J. F. Banas (50)  
9721 K. D. Boulttinghouse (10)  
Attn: W. E. Boyd  
J. E. Cannon  
R. L. Champion  
R. W. Harrigan  
B. J. Petterson  
S. Thunborg  
J. L. Todd, Jr.  
G. W. Treadwell  
9722 J. V. Otts  
9723 E. L. Burgess  
9724 E. C. Boes  
9725 R. H. Braasch  
9727 J. A. Leonard  
3141 J. L. Erickson (5)  
3151 W. L. Garner (3)  
3154-2 C. H. Dalin (25)  
(Unlimited Release  
for DOE/TIC)



## Sandia National Laboratories